Computer Vision

Lecture 3 – Structure-from-Motion

Prof. Dr.-Ing. Andreas Geiger

Autonomous Vision Group

University of Tübingen / MPI-IS

EBERHARD KARLS
UNIVERSITÄT
TÜBINGEN

ellis
European Laboratory for Learning and Intelligent Systems

Agenda

3.1 Preliminaries

3.2 Two-frame Structure-from-Motion

3.3 Factorization

3.4 Bundle Adjustment

3.1
Preliminaries

Camera Calibration

Camera Calibration

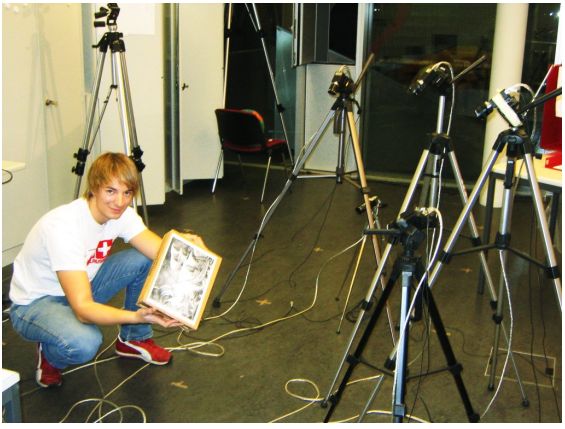

- **Camera calibration** is the process of finding the **intrinsic/extrinsic parameters**
- Most commonly, a **known calibration target** (image, checkerboard) is used

Camera Calibration

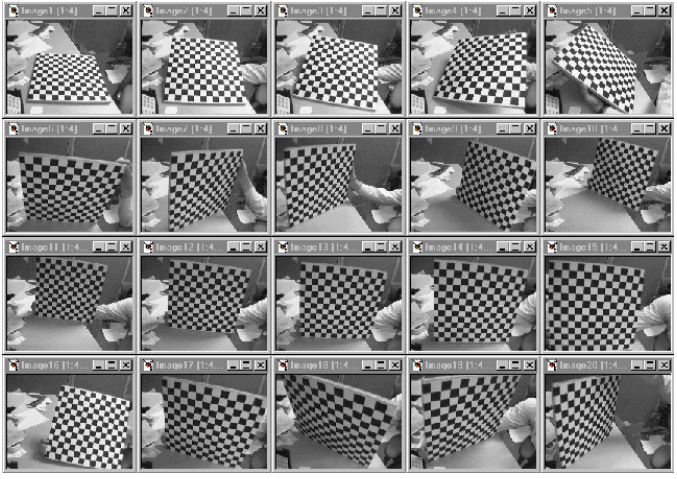

- First, the known calibration target is **captured in different poses**

Camera Calibration

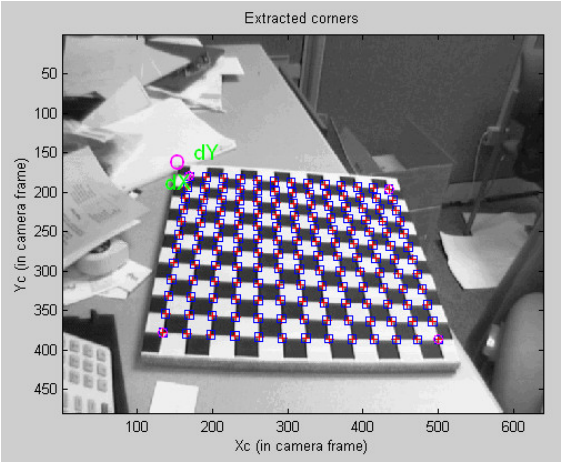

- Second, **features** (e.g., corners) on the target are detected in the images

Camera Calibration

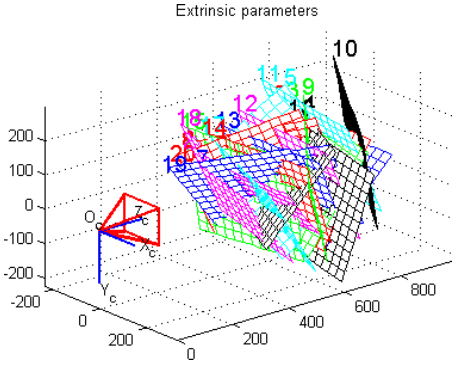

Finally, the **camera intrinsics and extrinsics** (=poses) are **jointly optimized:**

- **Closed-form solution** initializes all parameters except for distortion parameters
- **Non-linear optimization** of all parameters by minimizing reprojection errors

Zhang: A Flexible New Technique for Camera Calibration. TPAMI, 2000.

Camera Calibration

Remarks:

- There exists a variety of calibration techniques that are used in different settings
- These methods differ algorithmically, but also in the type of assumptions and calibration targets they use: 2D/3D targets, planes, vanishing points, etc.

Further Readings:

- `http://www.vision.caltech.edu/bouguetj/calib_doc/index.html`
- `https://docs.opencv.org/master/dc/dbb/tutorial_py_calibration.html`
- See also: Szeliski Book, Chapter 11.1

Zhang: A Flexible New Technique for Camera Calibration. TPAMI, 2000.

Feature Detection and Description

Point Features

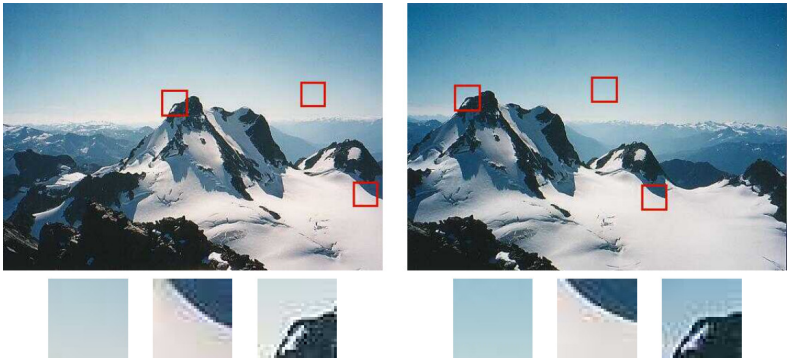

- **Point features** describe the appearance of **local, salient regions** in an image
- They can be used to **describe and match images** taken from different viewpoints
- They form the **basis of sparse 3D reconstruction methods** covered in this lecture

Image Credit: Rick Szeliski

Point Features

- Features should be **invariant** to **perspective** effects and **illumination**
- The same point should have **similar vectors** independent of pose/viewpoint
- Plain RGB/intensity patches will not have this property, we need something better

Lowe: Object Recognition from Local Scale-Invariant Features. ICCV, 1999.

Scale Invariant Feature Transform (SIFT)

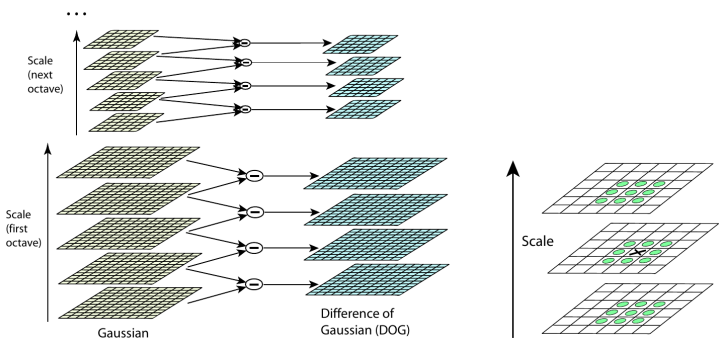

- SIFT constructs a **scale space** by iteratively filtering the image with a Gaussian
- Adjacent scales are subtracted, yielding **Difference of Gaussian (DoG)** images
- **Interest points** (=blobs) are detected as **extrema** in the resulting scale space

Lowe: Object Recognition from Local Scale-Invariant Features. ICCV, 1999.

Scale Invariant Feature Transform (SIFT)

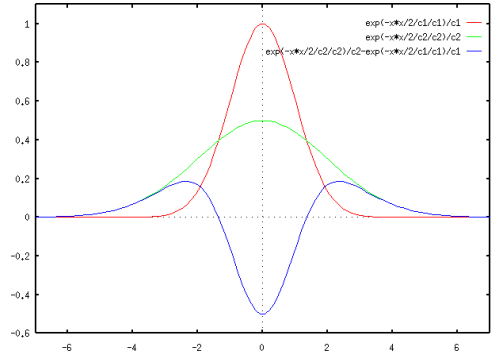

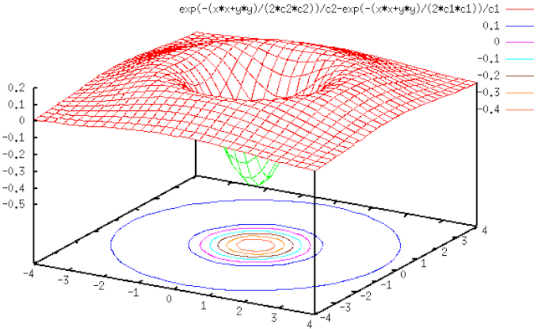

- SIFT constructs a **scale space** by iteratively filtering the image with a Gaussian
- Adjacent scales are subtracted, yielding **Difference of Gaussian (DoG)** images
- **Interest points** (=blobs) are detected as **extrema** in the resulting scale space

Lowe: Object Recognition from Local Scale-Invariant Features. ICCV, 1999.

Scale Invariant Feature Transform (SIFT)

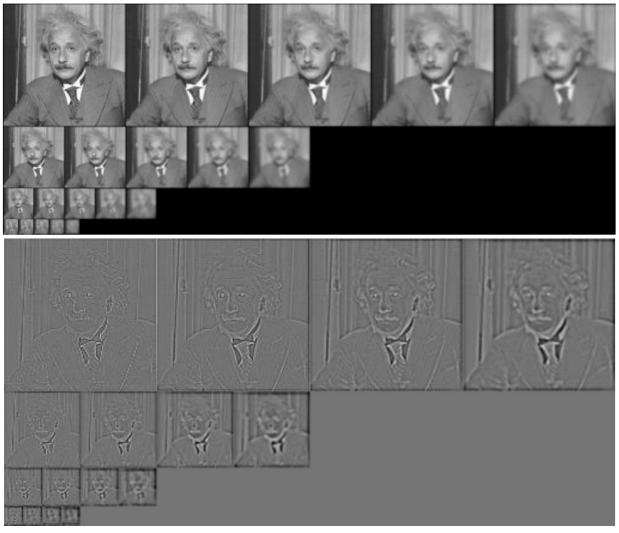

Lowe: Object Recognition from Local Scale-Invariant Features. ICCV, 1999.

Scale Invariant Feature Transform (SIFT)

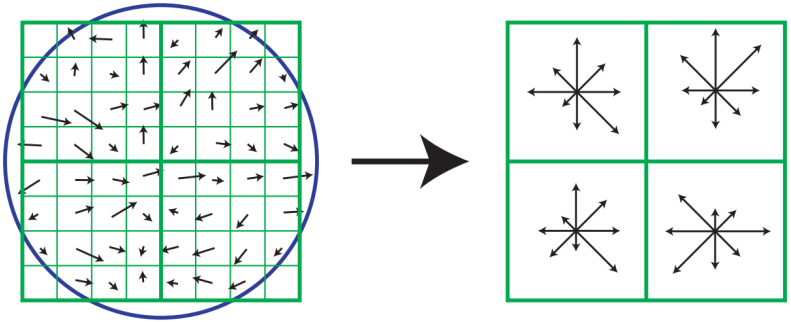

- SIFT **rotates** the descriptor to **align with the dominant gradient orientation**
- **Gradient histograms** are computed for local sub-regions of the descriptor
- All histograms are concatenated and normalized to form a **128D feature vector**

Lowe: Object Recognition from Local Scale-Invariant Features. ICCV, 1999.

Feature Detection and Description

- Many algorithms for feature detection and description have been developed, e.g., SIFT, SURF, U-SURF, BRISK, ORB, FAST, and recently deep learning based ones
- SIFT was a **seminal** work due to its invariance and robustness which revolutionized recognition and in particular matching and enabled the development of large-scale SfM techniques which we discuss in this lecture
- Despite >20 years old, SIFT is **still used today** (e.g., in the SfM pipeline COLMAP)
- Feature correspondences can be retrieved with **efficient nearest neighbor search**
- **Ambiguous matches** are typically **filtered** by computing the ratio of distance from the closest neighbor to the distance of the second closest
- A large ratio (>0.8) indicates that the found match might not be the correct one

Scale Invariant Feature Transform (SIFT)

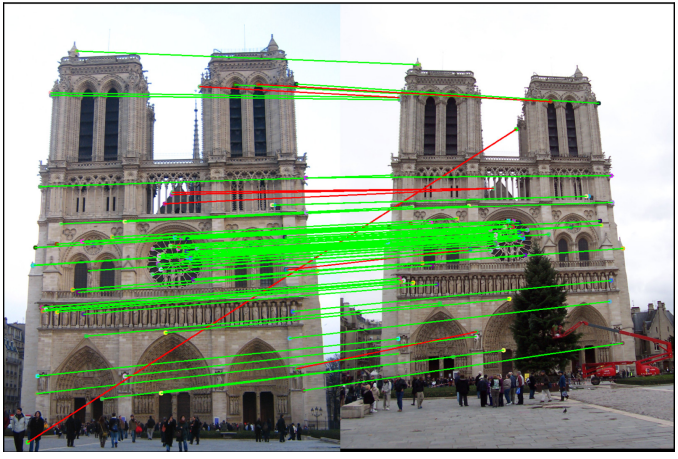

- Example of two images with SIFT correspondences (green: correct, red: wrong)

Image Credits: James Hays

3.2
Two-frame Structure-from-Motion

Epipolar Geometry

Epipolar Geometry

Goal: Recovery of camera pose (and 3D structure) from image correspondences.
The required relationships are described by the two-view **epipolar geometry.**

- Let $\mathbf{R}$ and $\mathbf{t}$ denote the relative pose between **two perspective cameras**
- A 3D point $\mathbf{x}$ is projected to pixel $\bar{\mathbf{x}}_1$ in image 1 and to pixel $\bar{\mathbf{x}}_2$ in image 2
- The 3D point $\mathbf{x}$ and the two camera centers span the **epipolar plane**
- The correspondence of pixel $\bar{\mathbf{x}}_1$ in image 2 must lie on the **epipolar line** $\tilde{\mathbf{l}}_2$ in image 2
- All epipolar lines pass through the **epipole**

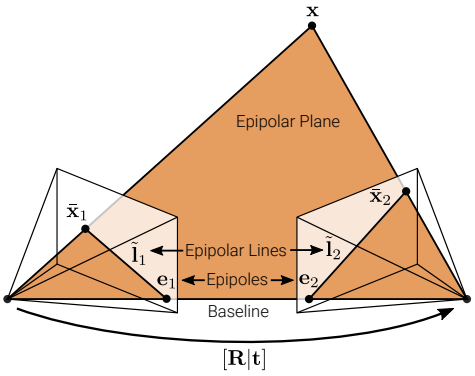

Epipolar Geometry

Let $\mathbf{K}_i \in \mathbb{R}^{3\times3}$ denote the **camera matrix** of camera i.

Let $\tilde{\mathbf{x}}_i = \mathbf{K}_i^{-1}\,\bar{\mathbf{x}}_i$ denote the **local ray direction** of pixel $\bar{\mathbf{x}}_i$ in camera i. We have:

$$\tilde{\mathbf{x}}_2 \;\propto\; \mathbf{x}_2 \;=\; \mathbf{R}\,\mathbf{x}_1 + \mathbf{t} \;\propto\; \mathbf{R}\,\tilde{\mathbf{x}}_1 + s\,\mathbf{t}$$

Taking the **cross product** of both sides with $\mathbf{t}$ we obtain:

$$[\mathbf{t}]_\times \tilde{\mathbf{x}}_2 \;\propto\; [\mathbf{t}]_\times \mathbf{R}\,\tilde{\mathbf{x}}_1$$

Taking the **dot product** of both sides with $\tilde{\mathbf{x}}_2^\top$ yields (triple product):

$$\tilde{\mathbf{x}}_2^\top [\mathbf{t}]_\times \mathbf{R}\,\tilde{\mathbf{x}}_1 \;\propto\; \tilde{\mathbf{x}}_2^\top [\mathbf{t}]_\times \tilde{\mathbf{x}}_2 = 0 \quad\Rightarrow\quad \tilde{\mathbf{x}}_2^\top [\mathbf{t}]_\times \mathbf{R}\,\tilde{\mathbf{x}}_1 = 0$$

Remark: The symbol $\propto$ denotes proportionality.

Epipolar Geometry

We arrive at the **epipolar constraint**

$$\tilde{\mathbf{x}}_2^\top \tilde{\mathbf{E}}\, \tilde{\mathbf{x}}_1 = 0$$

with **essential matrix:**

$$\tilde{\mathbf{E}} = [\mathbf{t}]_\times \mathbf{R}$$

$\tilde{\mathbf{E}}$ maps a point $\tilde{\mathbf{x}}_1$ in image 1 to the corresponding **epipolar line in image 2**

$$\tilde{\mathbf{l}}_2 = \tilde{\mathbf{E}}\, \tilde{\mathbf{x}}_1$$

as $\tilde{\mathbf{x}}_2^\top \tilde{\mathbf{l}}_2 = 0$.Similarly, by transposition, we obtain the **epipolar line in image 1:**

$$\tilde{\mathbf{l}}_1 = \tilde{\mathbf{E}}^\top \tilde{\mathbf{x}}_2$$

Epipolar Geometry

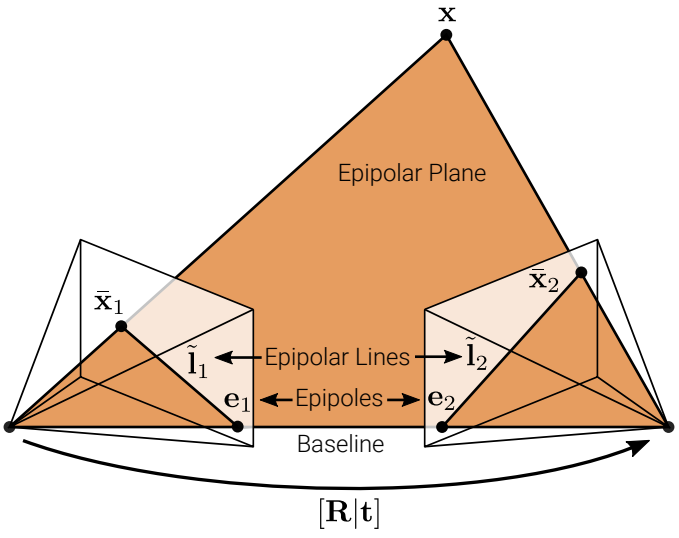

Epipolar Geometry

For any point $\tilde{\mathbf{x}}_1$ in the first image, the corresponding **epipolar line** $\tilde{\mathbf{l}}_2 = \tilde{\mathbf{E}}\,\tilde{\mathbf{x}}_1$ in the second image passes through the so-called **epipole** $\tilde{\mathbf{e}}_2$ which therefore satisfies

$$\tilde{\mathbf{e}}_2^\top \tilde{\mathbf{l}}_2 = \tilde{\mathbf{e}}_2^\top \tilde{\mathbf{E}}\,\tilde{\mathbf{x}}_1 = 0$$

for all $\tilde{\mathbf{x}}_1$. It follows that:

$$\tilde{\mathbf{e}}_2^\top \tilde{\mathbf{E}} = \mathbf{0}$$

Thus, $\tilde{\mathbf{e}}_2^\top$ is the **left null-space** (left singular vector with singular value 0) of $\tilde{\mathbf{E}}$. Further:

$$\tilde{\mathbf{E}}\,\tilde{\mathbf{e}}_1 = \mathbf{0}$$

Thus, $\tilde{\mathbf{e}}_1^\top$ is the **right null-space** (right singular vector with singular value 0) of $\tilde{\mathbf{E}}$.

Estimating the Epipolar Geometry

We can **recover the essential matrix $\tilde{\mathbf{E}}$** from N **image correspondences** forming N homogeneous equations in the nine elements of $\tilde{\mathbf{E}}$:

$$\begin{array}{ccccccccc} & x_1\,x_2\,e_{11} & + & y_1\,x_2\,e_{12} & + & x_2\,e_{13} & & \\ + & x_1\,y_2\,e_{21} & + & y_1\,y_2\,e_{22} & + & y_2\,e_{23} & & \\ + & x_1\,e_{31} & + & y_1\,e_{32} & + & e_{33} & = & 0 \end{array}$$

As $\tilde{\mathbf{E}}$ is homogeneous we use **singular value decomposition** to constrain the scale.

Note that some terms are products of two image measurements and hence amplify measurement noise asymmetrically. Thus, the **normalized 8-point algorithm** whitens the observations to have zero-mean and unit variance before the calculation and back-transforms the matrix recovered by SVD accordingly.

Hartley: In Defense of the Eight-Point Algorithm. TPAMI, 1997.

Estimating the Epipolar Geometry

From $\tilde{\mathbf{E}}$, we can recover the **direction** $\hat{\mathbf{t}}$ of the **translation** vector $\mathbf{t}$. We have:

$$\hat{\mathbf{t}}^\top \tilde{\mathbf{E}} = \hat{\mathbf{t}}^\top [\mathbf{t}]_\times \mathbf{R} = \mathbf{0}$$

Thus, $\tilde{\mathbf{E}}$ is singular and we obtain $\hat{\mathbf{t}}$ as the left singular vector associated with singular value 0. In practice the singular value will not be exactly 0 due to measurement noise, and we choose the smallest one. The other two singular values are roughly equal.

The rotation matrix $\mathbf{R}$ can also be calculated, see Szeliski, Section 11.3 (p. 683).

Remark: The essential matrix has 5 DoF (3 for rotation $\mathbf{R}$, 2 for translation direction $\hat{\mathbf{t}}$).

Estimating the Epipolar Geometry with unknown Intrinsics

If the camera calibration $\mathbf{K}_i$ is unknown, we cannot use the local ray directions $\tilde{\mathbf{x}}_i = \mathbf{K}_i^{-1}\,\bar{\mathbf{x}}_i$ as we only know the pixel coordinates $\bar{\mathbf{x}}_i$. The essential matrix becomes

$$\tilde{\mathbf{x}}_2^\top \tilde{\mathbf{E}}\,\tilde{\mathbf{x}}_1 = \bar{\mathbf{x}}_2^\top \mathbf{K}_2^{-\top} \tilde{\mathbf{E}}\,\mathbf{K}_1^{-1} \bar{\mathbf{x}}_1 = \bar{\mathbf{x}}_2^\top \tilde{\mathbf{F}} \bar{\mathbf{x}}_1 = 0$$

where $\tilde{\mathbf{F}} = \mathbf{K}_2^{-\top} \tilde{\mathbf{E}}\,\mathbf{K}_1^{-1}$ is called the **fundamental matrix.** Like $\tilde{\mathbf{E}}$, $\tilde{\mathbf{F}}$ is (in absence of noise) rank two and the epipoles can be recovered in the same way. However, the intrinsic parameters cannot be directly determined, i.e., we obtain only a **perspective reconstruction** and not a metric one.

Additional information (vanishing points, constancy of $\mathbf{K}$ across time, zero skew, aspect ratio) can be used to upgrade a perspective reconstruction to a metric one.

The Fundamental Matrix Song: `https://www.youtube.com/watch?v=DgGV3182NTk`

Epipolar Geometry

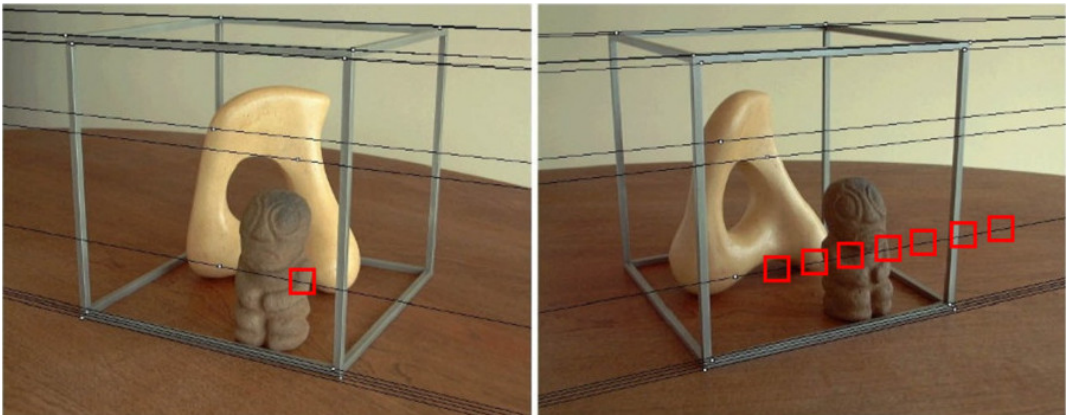

- **Epipolar lines** for two real images based on estimated epipolar geometry
- Note that corresponding points lie on the corresponding epipolar lines

Triangulation

Triangulation

Given the camera intrinsics and extrinsics, how can we recover 3D geometry?

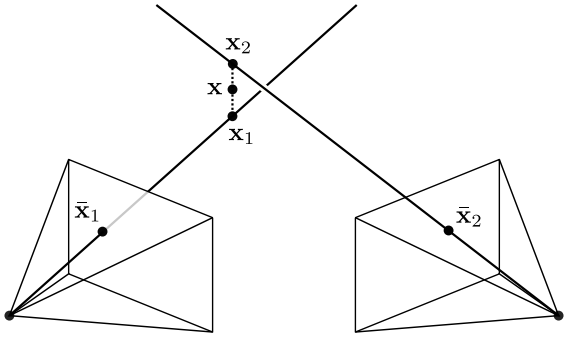

Given noisy 2D image observations $\bar{\mathbf{x}}_1$ and $\bar{\mathbf{x}}_2$, the two rays might not intersect in one point. We like to recover the 3D point $\mathbf{x}$ that (in some sense) is closest to the two rays.

Triangulation

Let $\tilde{\mathbf{x}}_i^s = \tilde{\mathbf{P}}_i \, \tilde{\mathbf{x}}_w$ denote the projection of a 3D world point $\tilde{\mathbf{x}}_w$ onto the image of the i'th camera $\tilde{\mathbf{x}}_i^s$. As both sides are homogeneous, they have the same direction but may differ in magnitude. To account for this, we consider the cross product $\bar{\mathbf{x}}_i^s \times \tilde{\mathbf{P}}_i \, \tilde{\mathbf{x}}_w = \mathbf{0}$. Using $\tilde{\mathbf{p}}_{ik}^\top$ to denote the k'th row of the i'th camera's projection matrix $\tilde{\mathbf{P}}_i$, we obtain:

$$\underbrace{\begin{bmatrix} x_i^s \, \tilde{\mathbf{p}}_{i3}^\top - \tilde{\mathbf{p}}_{i1}^\top \\ y_i^s \, \tilde{\mathbf{p}}_{i3}^\top - \tilde{\mathbf{p}}_{i2}^\top \end{bmatrix}}_{\mathbf{A}_i} \tilde{\mathbf{x}}_w = \mathbf{0}$$

Stacking $N \geq 2$ observations of a point, we obtain a linear system $\mathbf{A}\tilde{\mathbf{x}}_w = \mathbf{0}$. As $\tilde{\mathbf{x}}_w$ is homogeneous this leads to a constrained least squares problem. The solution to this problem is the **right singular vector** corresponding to the smallest singular value of $\mathbf{A}$. This is the **Direct Linear Transformation** we are already familiar with from Lecture 2.

Triangulation

Reprojection Error Minimization:

- While DLT often works well, it is not invariant to perspective transformations
- The gold standard is to minimize the reprojection error using numerical methods:

$$\bar{\mathbf{x}}_w^* = \underset{\bar{\mathbf{x}}_w}{\operatorname{argmin}} \sum_{i=1}^{N} \|\bar{\mathbf{x}}_i^s(\bar{\mathbf{x}}_w) - \bar{\mathbf{x}}_i^o\|_2^2 \qquad \text{with observation } \bar{\mathbf{x}}_i^o$$

- This allows to take measurement noise appropriately into account
- The minimum can also be obtained in closed form as the solution of a sixth degree polynomial, see Hartley & Zisserman, Section 12.5 for details

Triangulation Uncertainty

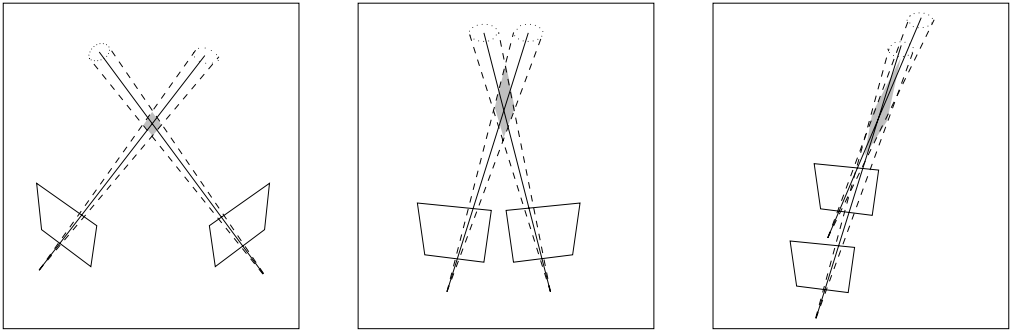

Triangulation works differently well depending on the relative camera pose:

- **Uncertainty** (shaded region) increases as the rays become more parallel
- **Tradeoff:** feature matching easier for nearby views, but triangulation is harder

3.3
Factorization

Orthographic Factorization

How can we use more than two views for structure-from-motion?

Let $\mathcal{W} = \{(x_{ip}, y_{ip}) \,|\, i = 1, \ldots, N,\ p = 1, \ldots, P\}$ denote P feature points tracked over N frames. Given $\mathcal{W}$ and assuming **orthographic projection,** our goal is to recover both **camera motion** (rotation) and the **structure** (3D points $\mathbf{x}_p$ corresponding to (x_{ip}, y_{ip})):

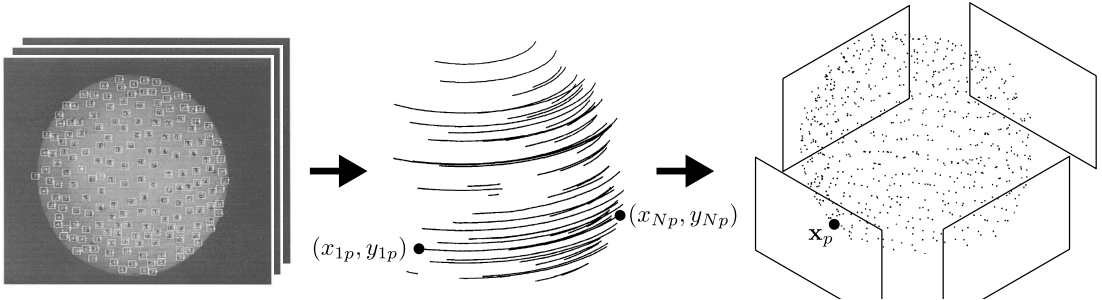

Tomasi and Kanade: Shape and motion from image streams under orthography: a factorization method. IJCV, 1992.

Orthographic Factorization

Under **orthographic projection,** a 3D point $\mathbf{x}_p$ maps to a pixel (x_{ip}, y_{ip}) in frame i as:

$$x_{ip} = \mathbf{u}_i^\top (\mathbf{x}_p - \mathbf{t}_i)$$
$$y_{ip} = \mathbf{v}_i^\top (\mathbf{x}_p - \mathbf{t}_i)$$

Without loss of generality, we assume that the **3D coordinate system** is at the center:

$$\frac{1}{P}\sum_{p=1}^{P} \mathbf{x}_p = 0$$

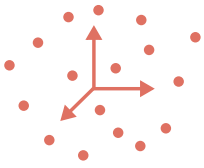

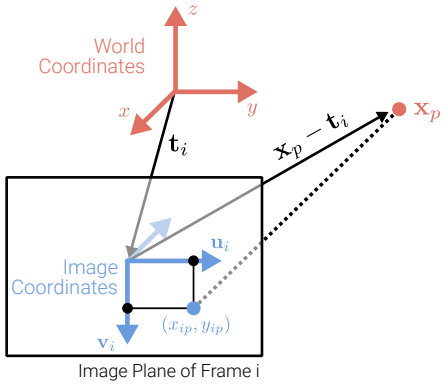

Tomasi and Kanade: Shape and motion from image streams under orthography: a factorization method. IJCV, 1992.

Orthographic Factorization

Let (x_{ip}, y_{ip}) denote the 2D location of feature p in frame i. Centering the features per frame (zero-mean) and collecting them yields the **centered measurement matrix $\tilde{\mathbf{W}}$**:

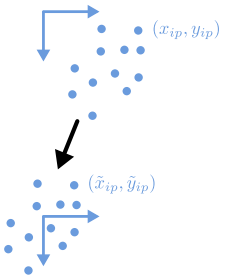

$$\tilde{x}_{ip} = x_{ip} - \frac{1}{P}\sum_{q=1}^{P} x_{iq}$$

$$\tilde{y}_{ip} = y_{ip} - \frac{1}{P}\sum_{q=1}^{P} y_{iq}$$

$$\tilde{\mathbf{W}} = \begin{bmatrix} \tilde{x}_{11} & \dots & \tilde{x}_{1P} \\ \vdots & & \vdots \\ \tilde{x}_{N1} & \dots & \tilde{x}_{NP} \\ \tilde{y}_{11} & \dots & \tilde{y}_{1P} \\ \vdots & & \vdots \\ \tilde{y}_{N1} & \dots & \tilde{y}_{NP} \end{bmatrix}$$

Remark: Here, the ˜ notation denotes centered, not homogeneous coordinates.

Tomasi and Kanade: Shape and motion from image streams under orthography: a factorization method. IJCV, 1992.

Orthographic Factorization

As $x_{ip} = \mathbf{u}_i^\top (\mathbf{x}_p - \mathbf{t}_i)$, the **centered image x-coordinate** is given by:

$$\begin{aligned}
\tilde{x}_{ip} &= x_{ip} - \frac{1}{P}\sum_{q=1}^{P} x_{iq} \\
&= \mathbf{u}_i^\top (\mathbf{x}_p - \mathbf{t}_i) - \frac{1}{P}\sum_{q=1}^{P} \mathbf{u}_i^\top (\mathbf{x}_q - \mathbf{t}_i) \\
&= \mathbf{u}_i^\top (\mathbf{x}_p - \mathbf{t}_i) - \mathbf{u}_i^\top \frac{1}{P}\sum_{q=1}^{P} \mathbf{x}_q + \mathbf{u}_i^\top \mathbf{t}_i \\
&= \mathbf{u}_i^\top \left(\mathbf{x}_p - \frac{1}{P}\sum_{q=1}^{P} \mathbf{x}_q \right) = \mathbf{u}_i^\top \mathbf{x}_p
\end{aligned}$$

Tomasi and Kanade: Shape and motion from image streams under orthography: a factorization method. IJCV, 1992.

Orthographic Factorization

We obtain a similar equation for **centered image y-coordinate**, thus we have:

$$\tilde{x}_{ip} = \mathbf{u}_i^\top \mathbf{x}_p \qquad \tilde{y}_{ip} = \mathbf{v}_i^\top \mathbf{x}_p$$

The **centered measurement matrix $\tilde{\mathbf{W}}$** can therefore be expressed as follows:

$$\tilde{\mathbf{W}} = \mathbf{R}\,\mathbf{X} \qquad \text{with} \qquad \tilde{\mathbf{W}} = \begin{bmatrix} \tilde{x}_{11} & \dots & \tilde{x}_{1P} \\ \vdots & & \vdots \\ \tilde{x}_{N1} & \dots & \tilde{x}_{NP} \\ \tilde{y}_{11} & \dots & \tilde{y}_{1P} \\ \vdots & & \vdots \\ \tilde{y}_{N1} & \dots & \tilde{y}_{NP} \end{bmatrix} \quad \mathbf{R} = \begin{bmatrix} \mathbf{u}_1^\top \\ \vdots \\ \mathbf{u}_N^\top \\ \mathbf{v}_1^\top \\ \vdots \\ \mathbf{v}_N^\top \end{bmatrix} \quad \mathbf{X} = \begin{bmatrix} \mathbf{x}_1 & \dots & \mathbf{x}_P \end{bmatrix}$$

Tomasi and Kanade: Shape and motion from image streams under orthography: a factorization method. IJCV, 1992.

Orthographic Factorization

$$\tilde{\mathbf{W}} = \mathbf{R}\,\mathbf{X} \qquad \text{with} \qquad \tilde{\mathbf{W}} = \begin{bmatrix} \tilde{x}_{11} & \dots & \tilde{x}_{1P} \\ \vdots & & \vdots \\ \tilde{x}_{N1} & \dots & \tilde{x}_{NP} \\ \tilde{y}_{11} & \dots & \tilde{y}_{1P} \\ \vdots & & \vdots \\ \tilde{y}_{N1} & \dots & \tilde{y}_{NP} \end{bmatrix} \quad \mathbf{R} = \begin{bmatrix} \mathbf{u}_1^\top \\ \vdots \\ \mathbf{u}_N^\top \\ \mathbf{v}_1^\top \\ \vdots \\ \mathbf{v}_N^\top \end{bmatrix} \quad \mathbf{X} = \begin{bmatrix} \mathbf{x}_1 & \dots & \mathbf{x}_P \end{bmatrix}$$

Here, $\mathbf{R}$ represents the camera **motion** (rotation), and $\mathbf{X}$ the **structure** of the 3D scene. As $\mathbf{R} \in \mathbb{R}^{2N \times 3}$ and $\mathbf{X} \in \mathbb{R}^{3 \times P}$, in the absence of noise, the centered measurement matrix $\tilde{\mathbf{W}}$ has at most **rank 3.** When adding noise, the matrix becomes **full rank.**

Tomasi and Kanade: Shape and motion from image streams under orthography: a factorization method. IJCV, 1992.

Orthographic Factorization

$$\underbrace{\tilde{\mathbf{W}}}_{\mathbb{R}^{2N\times P}} = \underbrace{\mathbf{R}}_{\mathbb{R}^{2N\times 3}} \underbrace{\mathbf{X}}_{\mathbb{R}^{3\times P}}$$

Given observed measurements with full rank $\hat{\mathbf{W}}$, we can find a rank 3 approximation minimizing $\|\hat{\mathbf{W}} - \tilde{\mathbf{W}}\|_F$ by using **singular value decomposition (SVD):**

$$\hat{\mathbf{W}} = \mathbf{U}\mathbf{\Sigma}\mathbf{V}^\top$$

We obtain the **rank 3 factorization** by considering the singular vectors corresponding to the top 3 singular values (the others should be small and capture noise primarily):

$$\underbrace{\hat{\mathbf{R}}}_{\mathbb{R}^{2N\times 3}} = \underbrace{\mathbf{U}}_{\mathbb{R}^{2N\times 3}} \underbrace{\mathbf{\Sigma}^{\frac{1}{2}}}_{\mathbb{R}^{3\times 3}} \qquad \underbrace{\hat{\mathbf{X}}}_{\mathbb{R}^{3\times P}} = \underbrace{\mathbf{\Sigma}^{\frac{1}{2}}}_{\mathbb{R}^{3\times 3}} \underbrace{\mathbf{V}^\top}_{\mathbb{R}^{3\times P}}$$

Tomasi and Kanade: Shape and motion from image streams under orthography: a factorization method. IJCV, 1992.

Orthographic Factorization

$$\hat{\mathbf{W}} = \mathbf{U}\mathbf{\Sigma}\mathbf{V}^\top \quad \Rightarrow \quad \hat{\mathbf{R}} = \mathbf{U}\mathbf{\Sigma}^{\frac{1}{2}} \qquad \hat{\mathbf{X}} = \mathbf{\Sigma}^{\frac{1}{2}}\mathbf{V}^\top$$

However, this decomposition is **not unique** as there exists a matrix $\mathbf{Q} \in \mathbb{R}^{3\times 3}$ such that

$$\hat{\mathbf{W}} = \mathbf{U}\mathbf{\Sigma}\mathbf{V}^\top = \hat{\mathbf{R}}\,\hat{\mathbf{X}} = (\hat{\mathbf{R}}\mathbf{Q})\,(\mathbf{Q}^{-1}\hat{\mathbf{X}})$$

To find $\mathbf{Q}$ we observe that the rows of $\mathbf{R}$ are unit vectors and the first half are orthogonal to the corresponding second half of $\mathbf{R}$. We obtain the **metric constraints:**

$$\hat{\mathbf{u}}_i^\top \mathbf{Q}\,(\hat{\mathbf{u}}_i^\top \mathbf{Q})^\top = \hat{\mathbf{u}}_i^\top \mathbf{Q}\,\mathbf{Q}^\top \hat{\mathbf{u}}_i = 1$$
$$\hat{\mathbf{v}}_i^\top \mathbf{Q}\,(\hat{\mathbf{v}}_i^\top \mathbf{Q})^\top = \hat{\mathbf{v}}_i^\top \mathbf{Q}\,\mathbf{Q}^\top \hat{\mathbf{v}}_i = 1$$
$$\hat{\mathbf{u}}_i^\top \mathbf{Q}\,(\hat{\mathbf{v}}_i^\top \mathbf{Q})^\top = \hat{\mathbf{u}}_i^\top \mathbf{Q}\,\mathbf{Q}^\top \hat{\mathbf{v}}_i = 0$$

Tomasi and Kanade: Shape and motion from image streams under orthography: a factorization method. IJCV, 1992.

Orthographic Factorization

Metric Constraints:

$$\hat{\mathbf{u}}_i^\top \mathbf{Q} \left(\hat{\mathbf{u}}_i^\top \mathbf{Q}\right)^\top = \hat{\mathbf{u}}_i^\top \mathbf{Q}\,\mathbf{Q}^\top \hat{\mathbf{u}}_i = 1$$
$$\hat{\mathbf{v}}_i^\top \mathbf{Q} \left(\hat{\mathbf{v}}_i^\top \mathbf{Q}\right)^\top = \hat{\mathbf{v}}_i^\top \mathbf{Q}\,\mathbf{Q}^\top \hat{\mathbf{v}}_i = 1$$
$$\hat{\mathbf{u}}_i^\top \mathbf{Q} \left(\hat{\mathbf{v}}_i^\top \mathbf{Q}\right)^\top = \hat{\mathbf{u}}_i^\top \mathbf{Q}\,\mathbf{Q}^\top \hat{\mathbf{v}}_i = 0$$

This gives us a large set of linear equations for the entries in the matrix $\mathbf{Q}\,\mathbf{Q}^\top$, from which the matrix $\mathbf{Q}$ can be recovered using standard Cholesky decomposition.

Tomasi and Kanade: Shape and motion from image streams under orthography: a factorization method. IJCV, 1992.

Orthographic Factorization

Algorithm:

1. Take measurements $\hat{\mathbf{W}}$
2. Compute SVD $\hat{\mathbf{W}} = \mathbf{U}\mathbf{\Sigma}\mathbf{V}^\top$ and keep the top 3 SVs
3. Define $\hat{\mathbf{R}} = \mathbf{U}\mathbf{\Sigma}^{\frac{1}{2}}$ and $\hat{\mathbf{X}} = \mathbf{\Sigma}^{\frac{1}{2}}\mathbf{V}^\top$
4. Compute $\mathbf{Q}\,\mathbf{Q}^\top$ and from this $\mathbf{Q}$
5. Compute $\mathbf{R} = \hat{\mathbf{R}}\mathbf{Q}$ and $\mathbf{X} = \mathbf{Q}^{-1}\hat{\mathbf{X}}$

Remarks:

- Advantage: **closed form solution** (determined up to an arbitrary global rotation)
- Disadvantage: **complete feature tracks** required ($\Rightarrow$ cannot handle occlusions)
- Solution: Apply to subsets of features/frames and propagate (see T&K, Sec. 5)

Tomasi and Kanade: Shape and motion from image streams under orthography: a factorization method. IJCV, 1992.

Orthographic Factorization: Results




Tomasi and Kanade: Shape and motion from image streams under orthography: a factorization method. IJCV, 1992.

Perspective Factorization

- Tomasi and Kanade's original factorization approach assume **orthography**
- Christy and Horaud (TPAMI, 1996) perform an initial orthographic reconstruction and then correct perspective in an iterative manner
- Triggs (CVPR, 1996) performs **projective factorization**, iteratively updating depth
- Even though inaccurate, factorization methods can provide a **good initialization** for iterative techniques such as bundle adjustment
- However, modern SfM approaches (e.g., COLMAP) often perform **incremental bundle adjustment,** initializing with a carefully selected two-view reconstruction and iteratively adding new images/cameras to the reconstruction

Christy and Horaud: Euclidean shape and motion from multiple perspective views by affine iterations. TPAMI, 1996.

3.4
Bundle Adjustment

Bundle Adjustment

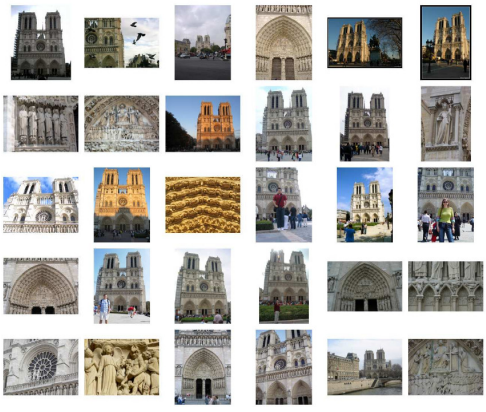

- **Goal: Optimize reprojection errors** (distance between observed feature and projected 3D point in image plane) **wrt. camera parameters and 3D point cloud**

Snavely, Seitz and Szeliski: Photo tourism: exploring photo collections in 3D. SIGGRAPH, 2006.

Bundle Adjustment

Let $\Pi = \{\pi_i\}$ denote the N cameras including their intrinsic and extrinsic parameters.
Let $\mathcal{X}_w = \{\mathbf{x}_p^w\}$ with $\mathbf{x}_p^w \in \mathbb{R}^3$ denote the set of P 3D points in world coordinates.
Let $\mathcal{X}_s = \{\mathbf{x}_{ip}^s\}$ with $\mathbf{x}_{ip}^s \in \mathbb{R}^2$ denote the image (screen) observations in all i cameras.

Bundle adjustment minimizes the reprojection error of all observations:

$$\Pi^*, \mathcal{X}_w^* = \underset{\Pi, \mathcal{X}_w}{\operatorname{argmin}} \sum_{i=1}^{N} \sum_{p=1}^{P} w_{ip} \left\| \mathbf{x}_{ip}^s - \pi_i(\mathbf{x}_p^w) \right\|_2^2$$

Here, w_{ip} indicates if point p is observed in image i and $\pi_i(\mathbf{x}_p^w)$ is the 3D-to-2D projection of 3D world point $\mathbf{x}_p^w$ onto the 2D image plane of the i'th camera, i.e.:

$$\pi_i(\mathbf{x}_p^w) = \begin{pmatrix} \tilde{x}_p^s / \tilde{w}_p^s \\ \tilde{y}_p^s / \tilde{w}_p^s \end{pmatrix} \quad \text{with} \quad \tilde{\mathbf{x}}_p^s = \mathbf{K}_i (\mathbf{R}_i \, \mathbf{x}_p^w + \mathbf{t}_i)$$

Bundle Adjustment

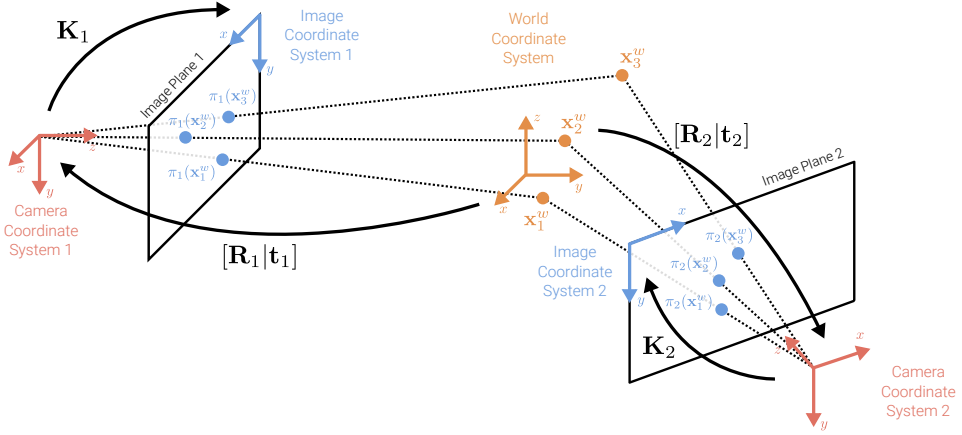

$\mathbf{K}_i$ and $[\mathbf{R}_i|\mathbf{t}_i]$ are the intrinsic and extrinsic parameters of π_i, respectively.

During bundle adjustment, we optimize $\{(\mathbf{K}_i, \mathbf{R}_i, \mathbf{t}_i)\}$ and $\{\mathbf{x}_p^w\}$ jointly.

Challenges of Bundle Adjustment

Initialization:

- The energy landscape of the bundle adjustment problem is highly **non-convex**
- A good **initialization** is crucial to avoid getting trapped in bad local minima
- As initializing all 3D points and cameras jointly is difficult (occlusion, viewpoint, matching outliers), **incremental bundle adjustment** initializes with a carefully selected two-view reconstruction and iteratively adds new images/cameras

Optimization:

- Given millions of features and thousands of cameras, large-scale bundle adjustment is **computationally demanding** (cubic complexity in #unknowns)
- Luckily, the problem is **sparse** (not all 3D points are observed in every camera), and efficient sparse implementations (e.g., Ceres) can be exploited in practice

Incremental Structure-from-Motion

Incremental Structure-from-Motion

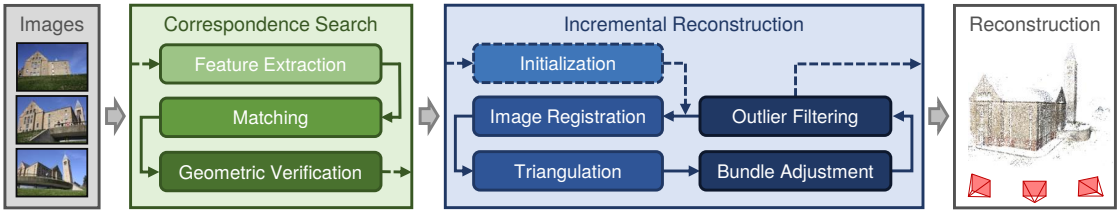

Feature matching and reconstruction pipeline (COLMAP):

- **Correspondence Search:** Find and match robust 2D features acroess images
- **Incremental Reconstruction:** Start with 2 views, incrementally add cameras

Schönberger and Frahm: Structure-from-Motion Revisited. CVPR, 2016.

Feature Extraction

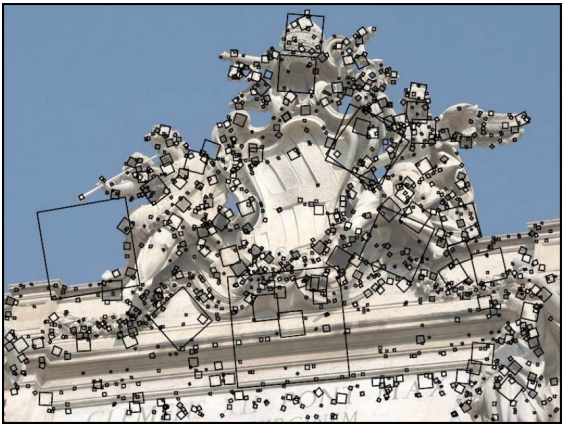

- **Detect features** (eg, SIFT, SURF, BRISK) in all input images

Feature Matching & Geometric Verification

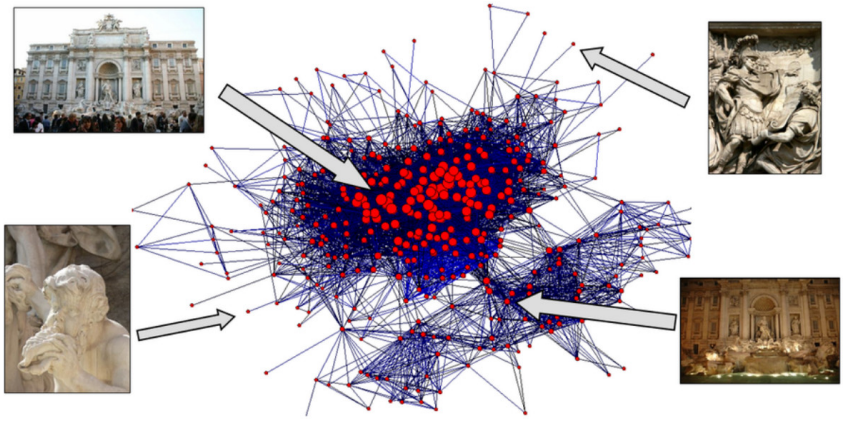

- Find **overlapping image pairs** and **associated feature correspondences**

Incremental Structure-from-Motion

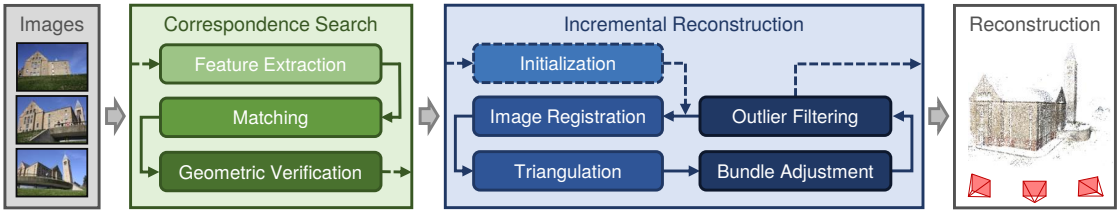

Feature matching and reconstruction pipeline (COLMAP):

- **Correspondence Search:** Find and match robust 2D features acroess images
- **Incremental Reconstruction:** Start with 2 views, incrementally add cameras

Schönberger and Frahm: Structure-from-Motion Revisited. CVPR, 2016.

Initialization

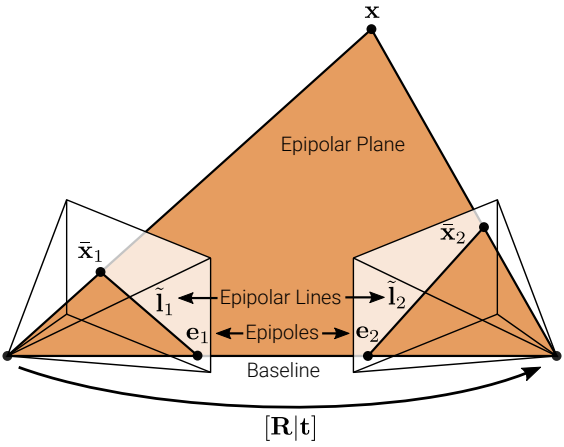

- Select **two views** with many correspondences and **estimate their geometry**

Image Registration

Find a **new image** with correspondences to the current set and **estimate camera pose:**

Let $\mathcal{X} = \{\bar{\mathbf{x}}_i^s, \bar{\mathbf{x}}_i^w\}_{i=1}^N$ be a set of N 3D-to-2D correspondences related by $\bar{\mathbf{x}}_i^s = \mathbf{P}\,\bar{\mathbf{x}}_i^w$. As the correspondence vectors are homogeneous, they have the same direction but differ in magnitude. Thus, the equation above can be expressed as $\bar{\mathbf{x}}_i^s \times \mathbf{P}\bar{\mathbf{x}}_i^w = \mathbf{0}$. Using the **Direct Linear Transform,** this can be written as a linear equation in the entries of $\mathbf{P}$. The solution to the constrained system (fixing $\mathbf{P}$'s scale) is given by SVD.

- Given that $\mathbf{P} = \mathbf{K}[\mathbf{R}|\mathbf{t}]$ and $\mathbf{K}$ is upper-triangular, both $\mathbf{K}$ and $\mathbf{R}$ can be easily obtained from the front 3×3 submatrix of $\mathbf{P}$ using standard RQ factorization
- If $\mathbf{K}$ is known, we can even estimate $\mathbf{P}$ from only three points (P3P algorithm)
- In practice, random sampling consensus (RANSAC) is used to remove outliers

Schönberger and Frahm: Structure-from-Motion Revisited. CVPR, 2016.

Triangulation

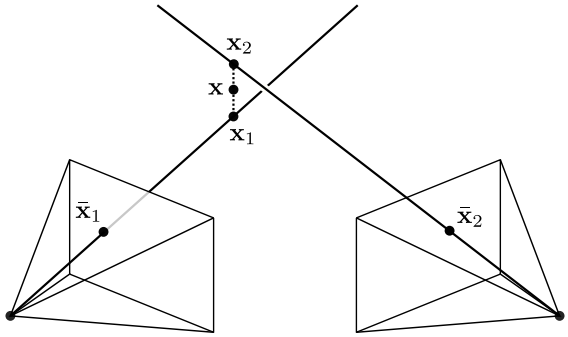

- Given the newly registered image, **new correspondences** can be **triangulated**
- In COLMAP, a robust triangulation method is proposed that handles outliers

Schönberger and Frahm: Structure-from-Motion Revisited. CVPR, 2016.

Bundle Adjustment & Outlier Filtering

Minimize reprojection error of all observations wrt. all cameras and 3D points:

$$\Pi^*, \mathcal{X}_w^* = \underset{\Pi, \mathcal{X}_w}{\operatorname{argmin}} \sum_{i=1}^{N} \sum_{p=1}^{P} w_{ip} \left\| \mathbf{x}_{ip}^s - \pi_i(\mathbf{x}_p^w) \right\|_2^2$$

- Since incremental SfM only affects the model locally, COLMAP performs **local BA** on the locally connected images, and **global BA** only once in a while for efficiency
- For solving the sparse large-scale optimization problem, COLMAP uses Ceres
- After each BA, observations with large reprojection errors and cameras with abnormal field of views or large distortion coefficients are removed

Schönberger and Frahm: Structure-from-Motion Revisited. CVPR, 2016.

Results and Applications

Building Rome in a Dav

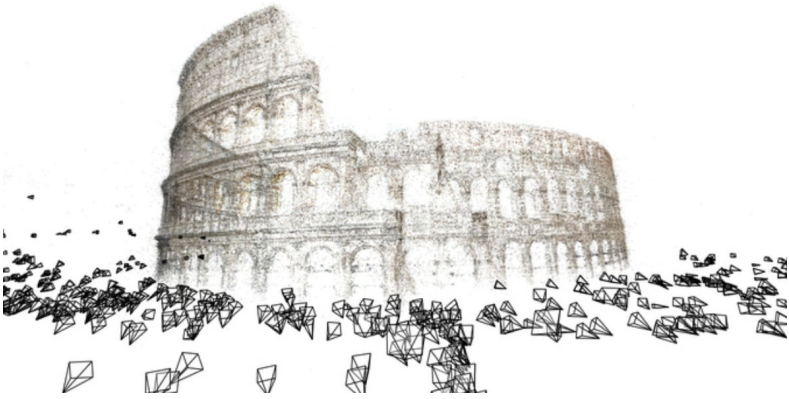

- First large-scale SfM from unstructured images: **Building Rome in a Day**

Agarwal, Snavely, Simon, Seitz and Szeliski: Building Rome in a day. ICCV, 2009.

COLMAP SfM

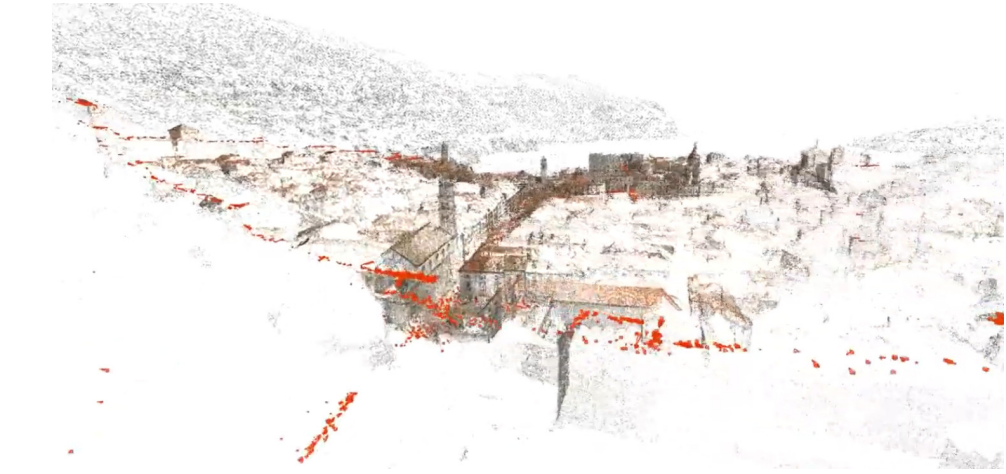

- **COLMAP** significantly improves accuracy and robustness compared to prior work

Schönberger and Frahm: Structure-from-Motion Revisited. CVPR, 2016.

COLMAP MVS

- COLMAP features a second **multi-view stereo stage** to obtain dense geometry

Schönberger, Zheng, Frahm and Marc Pollefeys: Pixelwise View Selection for Unstructured Multi-View Stereo. ECCV, 2016.

Photo Tourism

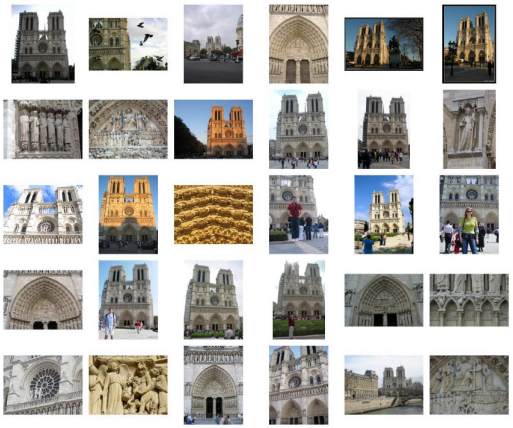

- **Photo Tourism / PhotoSynth** allows for exploring photo collections in 3D

Snavely, Seitz and Szeliski: Photo tourism: exploring photo collections in 3D. SIGGRAPH, 2006.

Parallel Tracking and Mapping (PTAM)

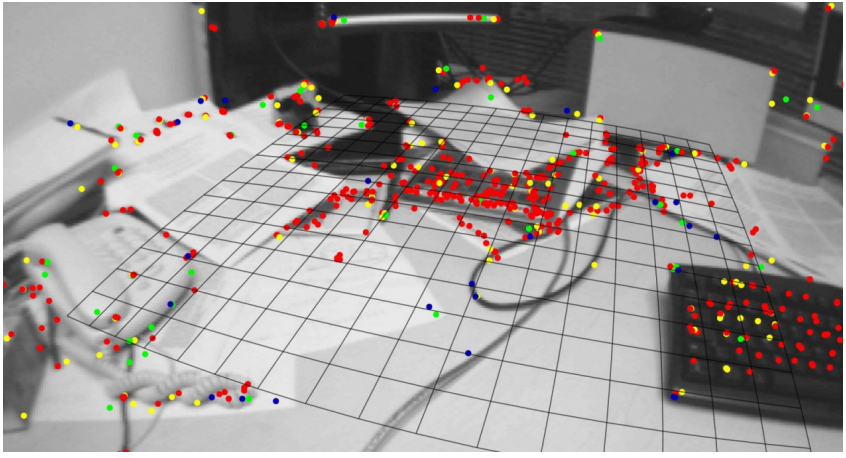

- **PTAM** demonstrates real-time tracking and mapping of small workspaces

Klein and Murray: Parallel Tracking and Mapping for Small AR Workspaces. ISMAR, 2007.

Match Move

- 2d3's automated camera motion tracker **Boujou** won an Emmy award in 2002

https://www.youtube.com/watch?v=JRL8_0vLcpw